

L A M S - 4 1 4
(LADC-297)
(MDDC-452) C.1

MEASUREMENT OF TRANSMITTANCE AND INELASTIC SCATTERING

CROSS SECTION FOR FAST NEUTRONS

Part II. Experimental Results

H. H. Pirschall*, M. E. Beaton**, W. C. Wright, E. R. Graves,
T. Jorgensen*, J. H. Manley***

Los Alamos Laboratory, Los Alamos, New Mexico

* Now at the University of Wisconsin

** Now at Washington University

*** Now at the University of Nebraska

**** Now on leave from Washington University

LOS ALAMOS NATIONAL LABORATORY



3 9338 00414 5438

MEASUREMENT OF TRANSPORT AND INELASTIC SCATTERING

CROSS SECTION FOR FAST NEUTRONS

Part II. Experimental Results

H. H. Barschall^{*}, M. E. Fattat^{**}, W. C. Bright, E. R. Graves,
T. Jorgensen^{***}, J. H. Manley^{****}

Los Alamos Laboratory, Los Alamos, New Mexico

Abstract

Measurements of poor geometry scattering and backscattering are described for neutrons of energies of 0.2, 0.6, 1.5, and 3 Mev. The following materials were investigated: C, Be, B¹⁰, B¹¹, BeO, Al, Fe, Ca, Co, Ni, Ta, Au and Pb. Values of the cross section for inelastic scattering and the transport cross section are given for these materials.



- * Now at the University of Wisconsin
- ** Now at Washington University
- *** Now at the University of Nebraska
- **** Now on leave from Washington University

MEASUREMENT OF TRANSPORT AND INELASTIC SCATTERING

CROSS SECTION FOR FAST NEUTRONS

Part II. Experimental Results

H. H. Barschall*, M. E. Battat**, W. C. Bright, E. R. Graves,
T. Jorgensen***, J. H. Manley****

Los Alamos Laboratory, Los Alamos, New Mexico

In the first part of the present paper¹ a method was described.

1. H. H. Barschall, J. H. Manley, V. F. Weisskopf, Phys. Rev.

This paper will be referred to as I.

which allows one to measure the transport and inelastic scattering cross sections for fast neutrons. In table I the scatterers used in these experiments are described.

MEASUREMENTS USING 0.2-Mev NEUTRONS

Source

0.2-Mev neutrons were obtained from the $\text{Li}(p,n)$ reaction by bombarding a Li target, about 15 Kev thick, with protons accelerated by the University of Wisconsin's electrostatic generator at Los Alamos. The proton current integrator served as a monitor for the neutron intensity.

* Now at the University of Wisconsin

** Now at Washington University

*** Now at the University of Nebraska

**** Now on leave from Washington University

At this energy the source is strongly anisotropic both in energy and intensity. This made it impossible to select an angle α_0 between the proton beam and the scattering axis such that corrections for anisotropic neutron flux were feasible for the 60° and 90° transmission geometries. Only measurements where the scatterer subtended a relatively small angle at the source could be carried out. In order to minimize the effect of the anisotropy of the source, all measurements were carried out with the scattering axis in the direction of the proton beam.

Detector

The most desirable detector for the scattering experiments described in this paper is one the response of which does not depend on the direction of incidence of the neutrons. For most of the experiments at 200 Kev a spherical proportional counter² was used. The outer electrode

2. The counter was designed and constructed by H. M. Agnew.

was a thin spherical copper shell, 3" in diameter. The inner electrode consisted of two circular wire loops with a common center arranged in two planes at right angles to each other. The chamber was filled to a pressure of 25 cm Hg with tank hydrogen, and operated at a voltage of approximately 2200. It was found experimentally that the response of the counter was spherically symmetric.

A measurement of the response of the counter as a function of neutron energy (see Fig. 1) showed that the energy sensitivity differed greatly from that expected for a gas recoil counter. This behavior is probably due to non-uniform gas amplification in different parts of the

counter. Consequently it was not possible to use the counter as a threshold detector and no effort was made to detect inelastic scattering which, at this neutron energy, was not expected to be important.

For the investigation of the scattering of Be, B and Al a cylindrical proportional counter filled with deuterium to a pressure of one atmos. was used.

Procedure

Three types of scattering experiments were carried out for 200-kev neutrons: transmission experiments in the geometry³ for which

3. Notations are defined in Part I (reference 1)

$\theta_m = 30^\circ$ ($D = 18.7''$, $\alpha_0 = 0^\circ$), back scattering experiments in the geometry shown in Fig. 2a, and ring scattering experiments in the geometry shown in Fig. 2b with an average scattering angle of 90° .

For the transmission experiments the number of recoils per monitor count in the presence of the scatterer and without the scatterer were counted. A paraffin cylinder, 80 cm long, was interposed between source and detector to measure the background due to room scattering. This background was subtracted from the data. The cross section was computed under the assumption of an exponential decrease of the neutron intensity in the scatterer. For the ring and backscattering experiments the recoil counts per monitor count were recorded for three conditions: with shadow cone and with scatterer, with cone and without scatterer, and without cone and without scatterer. From these data and the geometry the scattering cross section was computed⁴.

4. Calculation by P. Olum.

The method of computation is that used in a previous paper on elastic backscattering of d-d neutrons.⁵

5. J. H. Marley, et al., Phys. Rev.

Results

The cross sections obtained in these experiments are tabulated in Table II. In the case of BeO the cross section is given per molecule. All cross sections are given as if they applied over the total solid angle of 4π . For a poor geometry transmission experiment this means that the measured cross section is multiplied by $2/(\cos \theta_m + 1)$. All the data are based on at least six separate runs, and were taken simultaneously at three different biases of the discriminator. A measurable bias effect was observed only in C and BeO in the ring and backscattering geometry. This bias effect may be explained entirely by energy loss in elastic collisions. From the consistency of the individual runs the error in the measurements of the cross sections is estimated to be about five percent.

The data in Table II, except the transport cross sections, are not corrected for multiple scattering, nor for energy loss in elastic collisions.

MEASUREMENTS USING 0.6-Mev NEUTRONS

Source

0.6-Mev neutrons were obtained from the Li(p,n) reaction monitored by the current integrator. By measuring the response of the detector as a

function of the angle α it was found by successive approximations that the anisotropy of the source cancelled to within five percent if α_0 was chosen to be 60° , i.e., if the proton energy were such that 0.6-Mev neutrons were emitted from the target at an angle of 60° with respect to the proton beam.

Detector

The detector was a cylindrical proportional counter similar to that described by Coon and Nobles⁵, except that it contained no

5. J. H. Coon and R. A. Nobles, Rev. Sci. Inst.

radiator, and was filled with one atmos. of deuterium rather than an inert gas. Typical response curves determined experimentally for this counter for three different biases are plotted against neutron energy in Fig. 3.

According to the definitions given in I, biases are specified in terms of the neutron energy at which the response of the counter rises above background, but it should be noted that the effective average threshold is considerably higher. The lowest bias was chosen above the maximum pulse height due to gamma rays. The highest bias was limited by the counting rates.

The response of the counter was not isotropic. The sensitivity to neutrons incident at 30° with respect to the axis of the counter was 10 percent higher than the sensitivity to neutrons incident perpendicularly to the axis for the lowest bias. The corresponding figure for the highest bias was 20 percent. A correction for the anisotropic response of the counter was made in the evaluation.

Results

Poor geometry measurements were made for $\theta_m = 30^\circ, 60^\circ, \text{ and } 90^\circ$.

Backscattering experiments were carried out for an average scattering angle of 135° (see Fig. 2a). The results are tabulated in Table III. The errors of the measurements, apart from systematic errors, are again estimated to be about five percent. The data are not corrected for anisotropic response of the detector, multiple scattering, or energy loss in elastic collisions. The last column of Table III lists results computed for transport cross sections. These are corrected for anisotropic response of the detector and energy loss in elastic collisions. The values given in parentheses are not corrected for multiple scattering and are calculated according to the method described in I, while those given without parentheses are based on the accurate method to be described in Part III of this paper. The evaluation showed that the observed bias effect in the light elements can be explained entirely by elastic scattering. In none of the heavier elements was the bias effect sufficiently large to yield a measurement of inelastic scattering. Considering the error of the measurements, this corresponds to an upper limit of approximately $3 \times 10^{-25} \text{ cm}^2$ for the cross section of 0.6-Mev neutrons for inelastic scattering by the elements listed in Table III. The biases at which measurements are reported are different for different substances, partly because the measurements were carried out at different times over a period of over a year and the detecting equipment was altered during that period.

MEASUREMENTS USING 1.5-Mev NEUTRONS

Source

1.5-Mev neutrons were likewise obtained from the $\text{Li}(p,n)$ reaction. The angle α_0 was chosen to be 90° . The proton current integrator served as

a monitor. The Li target was about 70 kev thick which produces an energy spread of 80 kev in 1.5 Mev.

Detector

The detector was a spherical ionization chamber², 3" in diameter. The collecting electrode, a ball 1/4" in diameter, was mounted on a 1/8" brass rod in the center of the sphere. The chamber was filled with a mixture of 24 lbs/in² of argon and 12 lbs/in² of hydrogen. Under these conditions the range of a 1.5 Mev proton is about one inch. A negative collecting voltage of 2100 was applied to the outer shell. The sensitivity of the detector as a function of neutron energy at three biases is shown in Fig. 4. The response of the detector as a function of the angle of incidence of the neutrons was found to be uniform.

Results

In Table IV the results for poor geometry and backscattering experiments are listed. The last column of Table IV shows values of transport cross section, the results corrected for multiple scattering being given without parentheses while the results which do not take into account multiple scattering are given in parentheses.

Table V shows the results obtained in several ring scattering geometries (see Fig. 2b). The 135° ring scattering geometry should yield results identical with the disk backscattering geometry. The results for Pb in these two geometries (Table IV and V) are in good agreement indicating that the geometric shadow of the paraffin core defines the active ring on the disk scatterer.

The cross sections for the inelastic scattering of 1.5-Mev

neutrons are given in Table VI. For the light elements the energy degradation due to elastic collisions masks any inelastic scattering which might be present. Calculations⁴ showed that the bias effect observed in elements lighter than iron may be attributed entirely to elastic scattering, except in the case of aluminum where there is an indication of an inelastic cross section of 1 or 2×10^{-25} cm² which, however, is within the accuracy of the measurements. The cross sections computed taking into account multiple scattering are given without parentheses in Table VI, while cross sections which are not corrected for multiple scattering are shown in parentheses. The satisfactory agreement between the results obtained by the two methods in the case of Fe and Pb indicates that the effect of multiple scattering on the calculation of inelastic scattering cross sections is not appreciable for the scatterers used. For Fe and Pb the cross sections for inelastic scattering below the high bias could not be determined because different biases were used in the transmission and backscattering experiments. For the same reason the high bias data were not used in the calculation of transport cross sections.

MEASUREMENTS USING 3-Mev NEUTRONS

Source

3-Mev neutrons were obtained from the d-d reaction. A thick D₂O ice target was bombarded with unanalyzed 200-kev deuteron ions which were accelerated by means of a Cockcroft-Walton set. The accompanying $d(d,p)H^3$ reaction was used for monitoring the neutron intensity.

The measurements were at first carried out at an angle $\alpha_0 = 60^\circ$

in order to minimize the effect of the anisotropy of the neutron source. At this angle the neutron energy is approximately 2.8 Mev. It was found, however, that it was extremely difficult to carry out backscattering experiments in the geometry for which $\alpha_0 = 60^\circ$. The count due to the small number of backscattered neutrons was less than the background due to neutrons formed in parts of the accelerator other than the target. However, by carrying out the experiments in the forward direction ($\alpha_0 = 0^\circ$, neutron energy 3.1 Mev) the detector was shielded by the shadow-cone from the neutrons from spurious sources in the accelerator. All the backscattering experiments and some of the transmission experiments were carried out in this geometry. In this case the background was always smaller than the count due to the scatterer.

Detector

The detector was the same as the one used for the experiments at 1.5 Mev except that it was filled with a mixture of 2 atmos. of hydrogen and 4 atmos. of argon. Since no neutron source was available the energy of which could be varied continuously up to 3 Mev no direct determination of bias energies was possible. Instead, the counting rate as a function of bias was measured for 3-Mev neutrons. It was assumed that the extrapolation of the bias curve to zero counting rate would give the pulse height corresponding to the primary energy and that other bias energies could be obtained by taking a linear dependence of pulse height on neutron energy.

Results

In Table VII the results obtained at $\alpha_0 = 60^\circ$, neutron energy 2.8 Mev, are listed. Table VIII gives measurements carried out in the

forward direction. The latter require an appreciable correction for the anisotropy of the source. The correction was calculated from the measured response of the detector when it was moved on a circle around the source. The last column of Table VIII shows calculated transport cross sections. The calculation of the transport cross sections assumes that there is no significant difference in the cross sections between 2.8 and 3.1 Mev. The correction for the anisotropy of the source was applied. In view of the fact that energy sensitivity curves for the detector were not available, the calculation of the transport cross section for light elements is subject to considerable uncertainty. Only the data taken at the low bias were used for obtaining the transport cross section for C and BeO, since the effect of energy loss in elastic encounters will be least noticeable at the low bias. Only the values of σ_T given without parentheses are corrected for multiple scattering.

Table IX gives a summary of inelastic cross sections. The lack of knowledge of the energy sensitivity of the detector made it impossible to determine inelastic cross sections for light elements.

Acknowledgments

We are indebted to Professor J. H. Williams for allowing us to use the electrostatic generator and are grateful for the cooperation of the operating crews of the generator, in particular, Messrs. J. M. Blair, K. Greisen, A. O. Hanson, J. M. Hush, E. D. Klema, L. W. Seagondollar, R. F. Taschek and C. M. Turner. Messrs. H. V. Agnew, G. Foster, K. Kupferberg helped in the operation of the Cockcroft-Walton set. The electronic equipment used in the experiments was designed and constructed

by the Los Alamos electronics group under the direction of Dr. D. K. Froman and Mr. W. A. Higinbotham. Prof. V. F. Weisskopf and Mr. P. Olum gave advice and help on theoretical problems throughout the experiments.

Captions for Figures

Fig. 1. Response of the spherical proportional counter used for the detection of 200-Kev neutrons as a function of neutron energy.

Fig. 2. Geometry used in scattering experiments.

a. Backscattering from a disk

b. Scattering by a ring

Fig. 3. Response of the cylindrical proportional counter used for the detection of 600-Kev neutrons as a function of neutron energy.

Fig. 4. Response of the spherical ionization chamber used for the detection of 1.5-Mev neutrons as a function of neutron energy.

TABLE I

Scatterers used in experiments

Disks

No. of sample	Substance	Thickness of sample cm	Area cm ²	Mass kg	Atoms or molecules/cm ² x 10 ⁻²⁴	I.D. cm	O.D. cm
1	Be	2.54	506	2.39	0.318		
2	B(normal)	3.18	506	2.28	0.251		
3	B(80.5% B ¹⁰)	3.18	506	2.16	0.251		
4	C	1.27	506	0.981	0.0972		
5	C	3.81	506	3.09	0.306		
6	BeO	1.23	506	1.43	0.0680		
7	BeO	4.37	506	3.91	0.185		
8	BeO	4.44	506	3.12	0.149		
9	Al	2.54	506	3.58	0.153		
10	Fe	2.54	506	10.0	0.214		
11	Ni	2.54	506	11.7	0.237		
12	Co	2.54	506	10.8	0.219		
13	Cu	2.54	506	11.5	0.214		
14	Ta	2.54	506	21.0	0.137		
15	Au	2.54	506	24.9	0.150		
16	Pb	2.54	506	14.6	0.0836		

Rings

17	C	1.27	253	0.526	0.103	17.8	25.4
18	C	3.81	253	1.58	0.306	17.8	25.4
19	BeO	2.58	253	1.09	0.100	17.8	25.5
20	BeO	4.37	253	2.01	0.186	17.8	25.4
21	Fe	2.54	253	5.16	0.216	17.8	25.4
22	Pb	2.54	253	7.45	0.0836	17.8	25.4
23	Pb	2.54	322	9.36	0.0836	15.2	25.4

TABLE II

Scattering cross sections for 0.2-Mev NeutronsCross sections in 10^{-24} cm²

Sample No.	Material	30° geometry	90° ring geometry			135° back-scattering geometry			transport Cross Section
			Bias→100	medium	high	low	medium	high	
1	Be	4.5							
2	B	3.9							
3	B	4.7							
	B ¹⁰	2.3 (absorption subtracted)							
	B ¹¹	3.6							
4	C	4.1				2.7	2.3	1.9	
17	C		2.8	2.5	2.2				
6	BeO	6.9				4.6	3.9	3.4	
19	BeO		4.4	3.6	3.1				
9	Al	5.8							
10	Fe	3.2				2.5	2.4	2.4	
21	Fe		2.8	2.6	2.5				
15	Au	7.7				4.9	4.7	4.6	
16	Pb	7.6				5.9	5.8	6.0	
22	Pb		6.1	6.2	6.0				

TABLE III

Scattering cross section in 10^{-24} cm² for 0.6-Mev Neutrons

Bias in italics in KeV

Sample No.	Material	30° geometry	60° geometry			90° geometry			Backscattering			σ_t
			<i>190</i>	<i>300</i>	<i>450</i>	<i>190</i>	<i>300</i>	<i>450</i>	<i>190</i>	<i>300</i>	<i>450</i>	
1	Be	3.3	<i>2.7</i>	<i>3.3</i>	<i>3.9</i>	<i>2.8</i>	<i>4.0</i>	<i>5.0</i>	<i>2.1</i>	<i>1.2</i>		3.4
2	B	2.7	<i>1.9</i>	<i>2.5</i>	<i>2.9</i>	<i>1.8</i>	<i>2.2</i>	<i>2.9</i>	<i>1.4</i>	<i>0.8</i>		
3	B (80.5% B ¹⁰)	3.6	<i>3.0</i>	<i>3.5</i>	<i>3.8</i>	<i>3.1</i>	<i>3.8</i>	<i>4.4</i>	<i>1.4</i>	<i>0.7</i>		
	B ¹⁰ (absorption subtracted)	3.0	<i>2.1</i>	<i>2.5</i>	<i>2.9</i>	<i>1.7</i>	<i>2.3</i>	<i>3.0</i>	<i>1.4</i>	<i>0.7</i>		3.9 (includes absorption)
	B ¹¹	2.4	<i>1.6</i>	<i>1.9</i>	<i>2.6</i>	<i>1.1</i>	<i>1.8</i>	<i>2.4</i>	<i>1.4</i>	<i>0.8</i>		2.1
5	C	3.0	<i>2.4</i>	<i>1.7</i>	<i>3.60</i>	<i>1.6</i>	<i>2.0</i>	<i>2.8</i>	<i>2.0</i>	<i>1.9</i>	<i>0.9</i>	2.8 (2.5)
6	BeO	6.2	<i>4.4</i>	<i>1.7</i>	<i>3.60</i>	<i>2.8</i>	<i>3.0</i>	<i>4.6</i>	<i>4.4</i>	<i>3.9</i>	<i>1.9</i>	5.0 (5.2)
9	Al	3.6	<i>2.7</i>	<i>2.5</i>	<i>3.75</i>	<i>1.8</i>	<i>1.8</i>	<i>2.2</i>	<i>2.5</i>	<i>2.4</i>	<i>2.1</i>	3.0 (3.1)
10	Fe	2.1	<i>1.6</i>	<i>1.5</i>	<i>3.60</i>	<i>0.8</i>	<i>1.0</i>	<i>1.0</i>	<i>1.7</i>	<i>1.6</i>	<i>1.4</i>	2.0 (1.8)
13	Cu	3.5	<i>2.7</i>	<i>2.5</i>	<i>3.75</i>	<i>1.8</i>	<i>1.8</i>	<i>2.2</i>	<i>3.0</i>	<i>3.0</i>	<i>2.9</i>	(3.5)
12	Co	3.4	<i>2.5</i>	<i>2.5</i>	<i>3.75</i>	<i>1.6</i>	<i>1.8</i>	<i>2.2</i>	<i>3.0</i>	<i>2.9</i>	<i>2.7</i>	(3.4)
16	Pb	5.1	<i>4.4</i>	<i>1.7</i>	<i>3.60</i>	<i>3.8</i>	<i>3.8</i>	<i>4.0</i>	<i>4.5</i>	<i>4.4</i>	<i>4.4</i>	4.4 (4.4)

TABLE IV

Scattering cross section in 10^{-24} cm² for 1.5-Mev Neutrons

Bias in italics in Kev

Sample No.	Material	30° geometry	60° geometry			90° geometry			Backscattering			σ_t
1	Be	1.9	<u>370</u> 1.5	<u>790</u> 1.6	<u>950</u> 1.7	<u>370</u> 1.2	<u>790</u> 2.0	<u>950</u> 2.2	<u>370</u> 0.9	<u>790</u> 0.2		1.4
2	B	2.0	<u>370</u> 1.9	<u>790</u> 2.1	<u>950</u> 2.4	<u>370</u> 1.8	<u>790</u> 2.6	<u>950</u> 2.9	<u>370</u> 1.5	<u>790</u> 0.8	<u>950</u> 0.5	
3	B (80.5% B ¹⁰)	2.0	<u>370</u> 1.8	<u>790</u> 2.1	<u>950</u> 2.2	<u>370</u> 2.0	<u>790</u> 2.5	<u>950</u> 2.6	<u>370</u> 1.0	<u>790</u> 0.5	<u>950</u> 0.2	
	B ¹⁰ (absorption subtracted)	1.4	<u>370</u> 1.0	<u>790</u> 1.1	<u>950</u> 1.3	<u>370</u> 0.8	<u>790</u> 1.2	<u>950</u> 1.3	<u>370</u> 0.9	<u>790</u> 0.4	<u>950</u> 0.1	2.1 (includes absorption)
	B ¹¹	2.0	<u>370</u> 2.0	<u>790</u> 2.1	<u>950</u> 2.4	<u>370</u> 1.8	<u>790</u> 2.6	<u>950</u> 3.0	<u>370</u> 1.7	<u>790</u> 0.9	<u>950</u> 0.6	2.2
5	C	1.8	<u>400</u> 1.6	<u>950</u> 1.8	<u>1300</u> 2.1	<u>400</u> 1.2	<u>950</u> 2.2	<u>1300</u> 2.8	<u>400</u> 1.6	<u>950</u> 0.6	<u>1100</u> 0.2	1.8 (1.8)
7	BeO	3.6	<u>400</u> 2.7	<u>950</u> 3.1	<u>1300</u> 3.9	<u>400</u> 2.4	<u>950</u> 4.0	<u>1300</u> 5.6	<u>400</u> 2.8	<u>950</u> 0.9	<u>1100</u> 0.4	3.6 (3.1)
9	Al	2.7	<u>370</u> 2.1	<u>790</u> 2.1	<u>950</u> 2.7	<u>370</u> 1.8	<u>790</u> 2.2	<u>950</u> 2.4	<u>370</u> 1.3	<u>790</u> 1.0	<u>950</u> 0.8	1.7
10	Fe	2.6	<u>400</u> 2.1	<u>950</u> 2.1	<u>1300</u> 2.7	<u>400</u> 2.0	<u>950</u> 3.0	<u>1300</u> 3.4	<u>400</u> 1.9	<u>950</u> 1.3	<u>1100</u> 1.1	2.2 (2.2)
11	Ni	2.7	<u>470</u> 2.3	<u>750</u> 2.1	<u>1150</u> 2.5	<u>470</u> 2.0	<u>750</u> 2.2	<u>1150</u> 2.6	<u>470</u> 2.0	<u>750</u> 1.9	<u>1150</u> 1.4	(2.3)
12	Cc	2.7	<u>470</u> 2.3	<u>750</u> 2.1	<u>1150</u> 2.7	<u>470</u> 2.2	<u>750</u> 2.4	<u>1150</u> 3.2	<u>470</u> 2.0	<u>750</u> 1.7	<u>1150</u> 1.2	(2.2)
13	Cu	2.6	<u>470</u> 2.4	<u>750</u> 2.1	<u>1150</u> 2.7	<u>470</u> 2.4	<u>750</u> 2.8	<u>1150</u> 3.4	<u>470</u> 1.6	<u>750</u> 1.3	<u>1150</u> 1.0	(2.2)
14	Ta	5.5	<u>470</u> 4.1	<u>750</u> 4.1	<u>1150</u> 4.8	<u>470</u> 5.0	<u>750</u> 6.2	<u>1150</u> 7.4	<u>470</u> 1.9	<u>750</u> 1.3	<u>1150</u> 0.9	(3.9)
16	Pb	3.8	<u>400</u> 3.2	<u>950</u> 3.1	<u>1300</u> 4.0	<u>400</u> 3.4	<u>950</u> 4.0	<u>1300</u> 4.0	<u>400</u> 3.1	<u>700</u> 2.6	<u>1100</u> 2.4	3.4 (3.1)

TABLE V

Scattering Cross Section in 10^{-24} cm² for 1.5 Mev Neutrons

Bias in italics in Kev

Sample No.	Material	90° ring geometry			115° ring geometry			135° ring geometry		
18	C	$\frac{400}{1.6}$	$\frac{950}{0.9}$	$\frac{1100}{0.6}$	$\frac{400}{1.5}$	$\frac{950}{0.6}$	$\frac{1100}{0.3}$			
20	BeO	$\frac{400}{2.8}$	$\frac{950}{1.4}$	$\frac{1100}{0.8}$	$\frac{400}{2.7}$	$\frac{950}{0.9}$	$\frac{1100}{0.4}$			
22	Pb	$\frac{400}{3.1}$	$\frac{950}{2.5}$	$\frac{1100}{0.4}$	$\frac{400}{4.0}$	$\frac{950}{3.5}$	$\frac{1100}{3.2}$			
23	Pb							$\frac{400}{3.1}$	$\frac{700}{2.6}$	$\frac{1100}{2.5}$

TABLE VI

Inelastic Scattering Cross Section for 1.5-Mev Neutrons

<u>Element</u>	Inelastic scattering cross section in 10^{-24} cm ²		
	<u>below low bias</u>	<u>below medium bias</u>	<u>below high bias</u>
Fe	0 (0)	0.6 (0.7)	
Ni	(0)	(0.1)	(0.6)
Co	(0)	(0.2)	(0.8)
Cu	(0.3)	(0.6)	(0.9)
Ta	(1.4)	(2.0)	(2.7)
Pb	0 (0)	0.4 (0.4)	

TABLE VII

Scattering Cross Section in 10^{-24} cm² for 2.8-Mev Neutrons

Sample No.	Material	30°	60°			90°		
		Bias (MeV) →	0.7	1.4	2.1	0.7	1.4	2.1
5	C	1.6	1.2	1.5	1.5	1.0	1.4	2.0
8	BeO	3.3	1.6	1.8	2.1	1.0	1.3	1.9
9	Al		1.7	1.9	2.4	0.8	1.4	2.2
10	Fe	2.8	1.7	2.1	2.5	1.4	2.2	3.2
15	Au		4.1	4.7	4.9	5.0	6.0	6.6
16	Pb	4.8	4.0	4.4	5.2	3.4	4.0	5.0

TABLE VIII

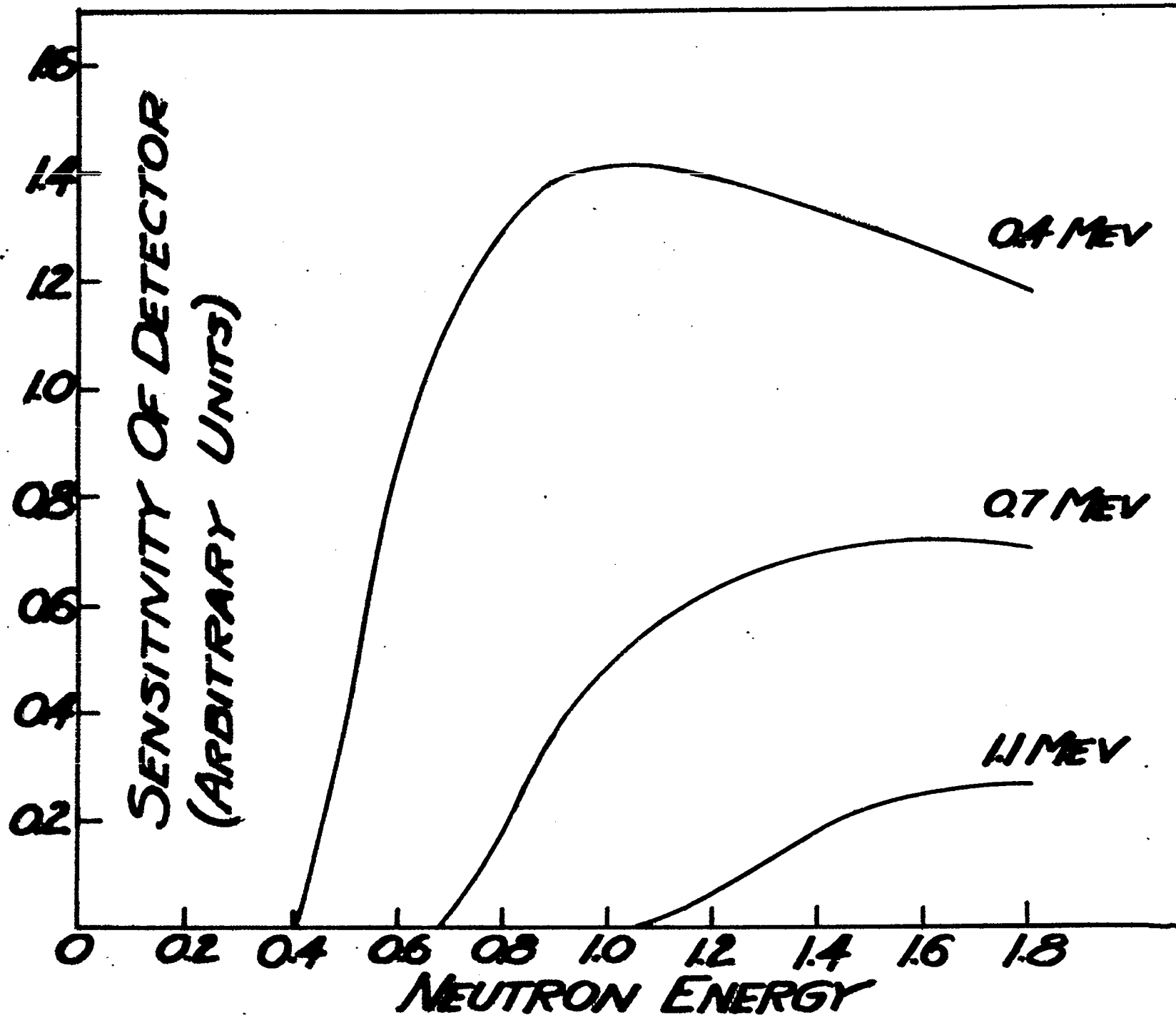
Scattering Cross Section in 10^{-24} cm² for 3-Mev Neutrons

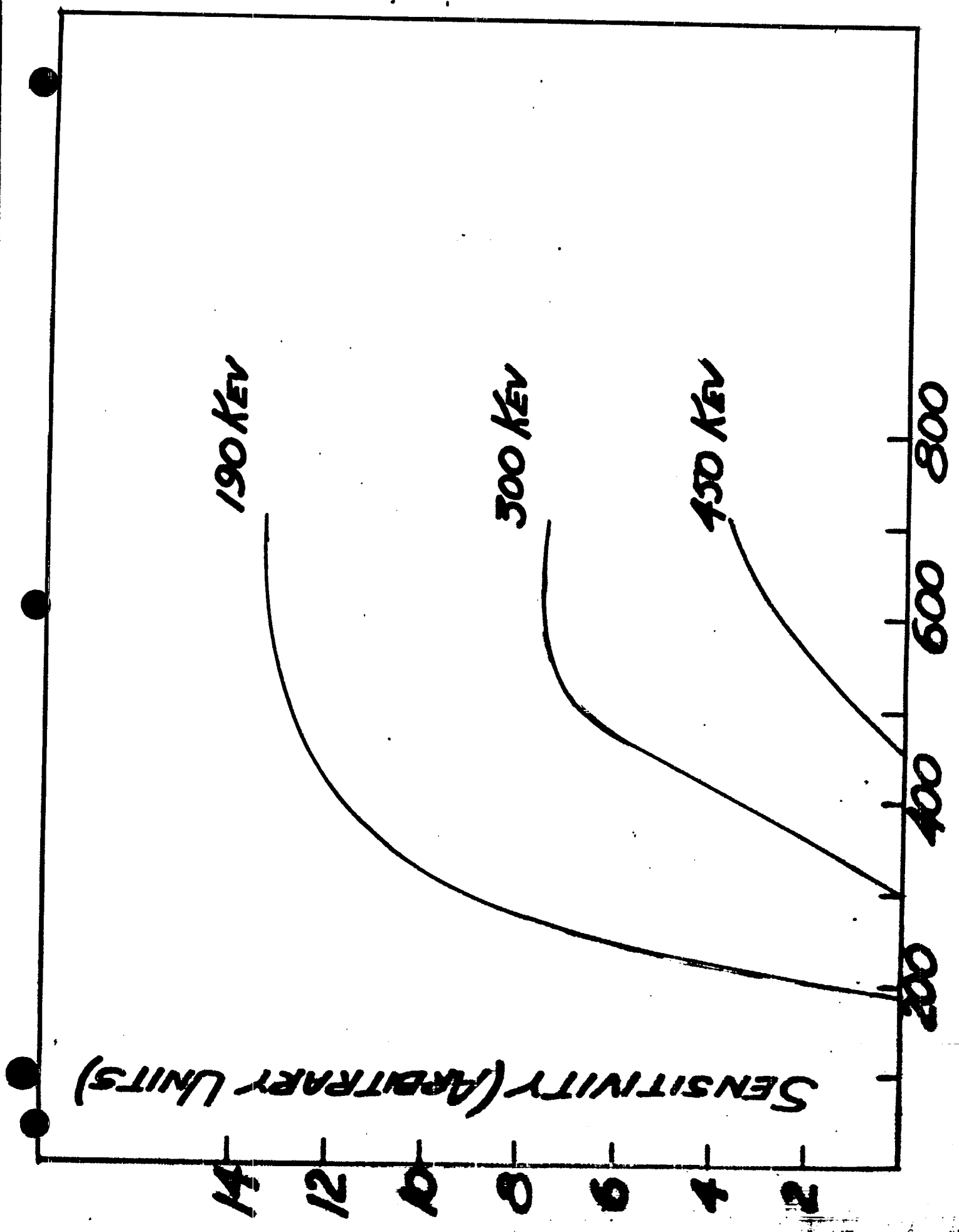
Sample No.	Material	30°			60°			90°			Backscattering			σ_t
		Bias(Mev) →			0.75	1.5	2.25	0.75	1.5	2.25	0.75	1.5	2.25	
1	Be	2.5												
2	B	1.7												
3	B	2.0												
	B ¹⁰	1.5 (absorption subtracted)												
	B ¹¹	1.6												
5	C							1.4	1.8	2.6	1.6	1.1		(1.7)
8	BeO							2.4	3.2	4.2	1.9	1.0		(2.7)
9	Al	2.4	1.6	1.7	1.9	1.4	1.6	2.0	1.0	0.7	0.4		1.4 (1.5)	
10	Fe					2.2	2.8	3.6	1.2	0.8	0.5		2.0 (2.2)	
12	Co	2.7							1.0	0.6	0.4		(2.1)	
13	Cu	2.6	2.1	2.5	2.7	2.6	3.6	3.6	1.0	0.5	0.3		(2.1)	
15	Au	4.8	4.3	4.7	4.8	5.6	6.6	7.0	0.9	0.4	0.3		(3.7)	
16	Pb	4.6	3.9	4.5	4.7	4.2	4.8	5.2	2.3	1.9	1.5		4.1 (3.6)	

TABLE IX

Inelastic Scattering Cross Section for 3-Mev Neutrons

Element	Inelastic scattering cross section in 10^{-24} cm^2		
	<u>below low bias</u>	<u>below medium bias</u>	<u>below high bias</u>
Fe	0.3 (0.5)	0.7 (1.0)	1.1 (1.4)
Cu	(0.6)	(1.3)	(1.5)
Au	(2.1)	(2.8)	(3.0)
Pb	0.7 (0.7)	1.2 (1.2)	1.6 (1.6)





SENSITIVITY (ARBITRARY UNITS)

NEUTRON ENERGY (KEV)

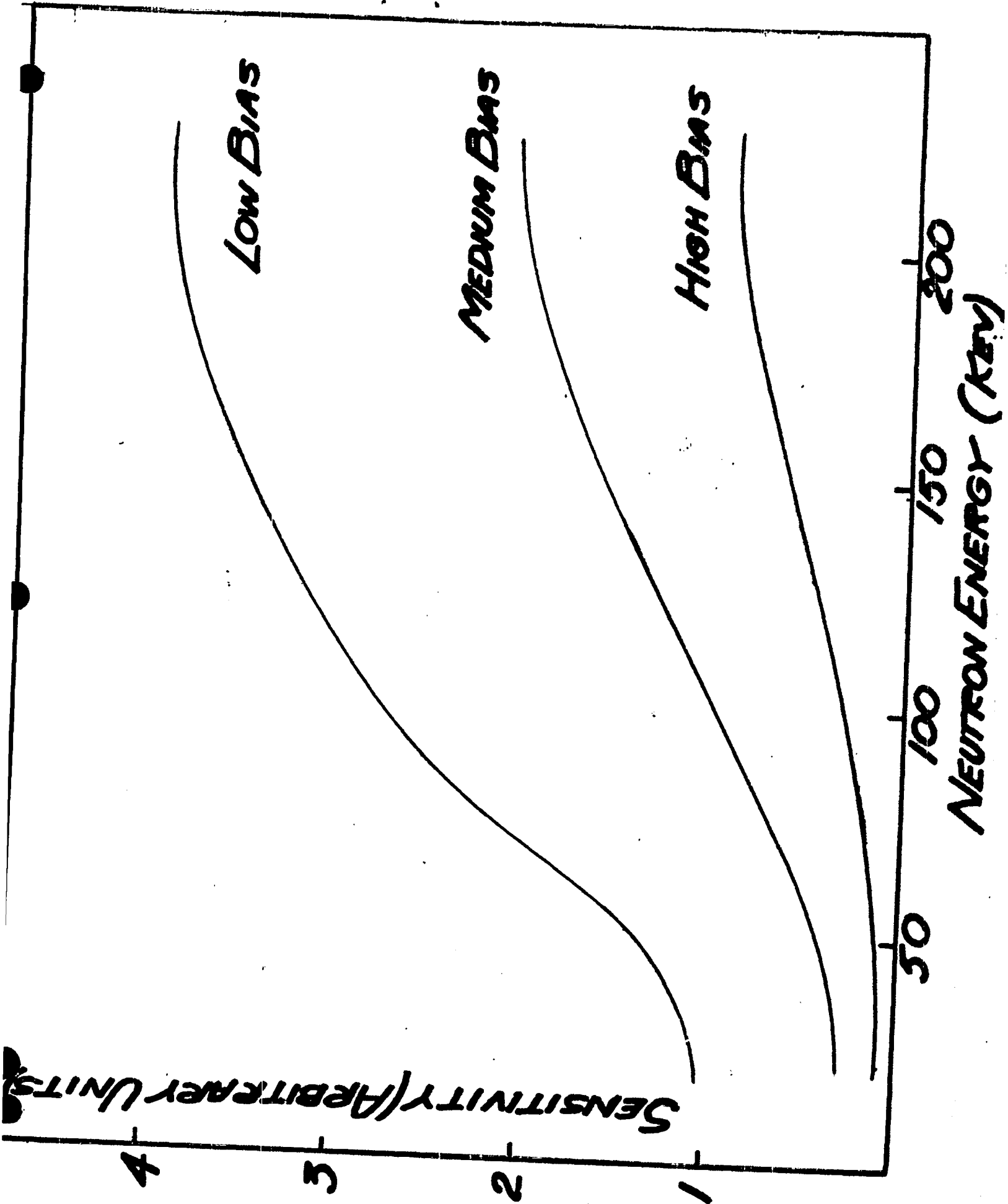
190 KEV

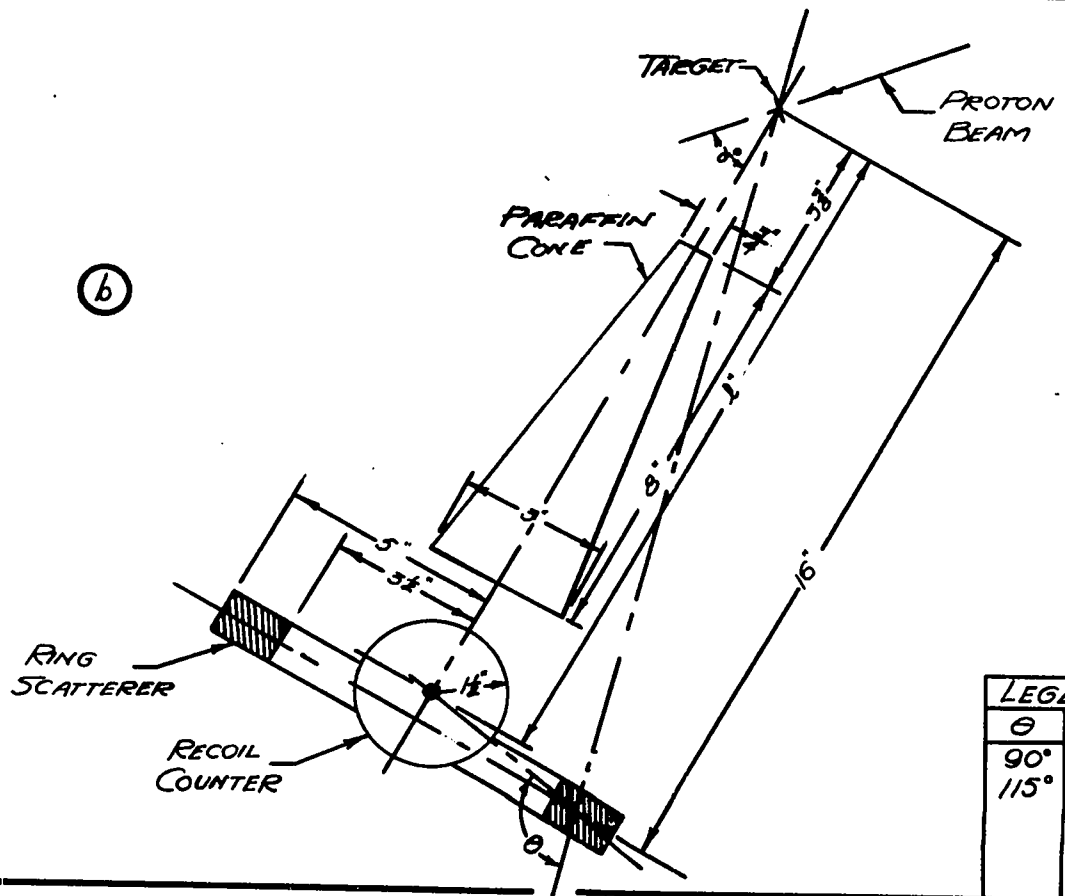
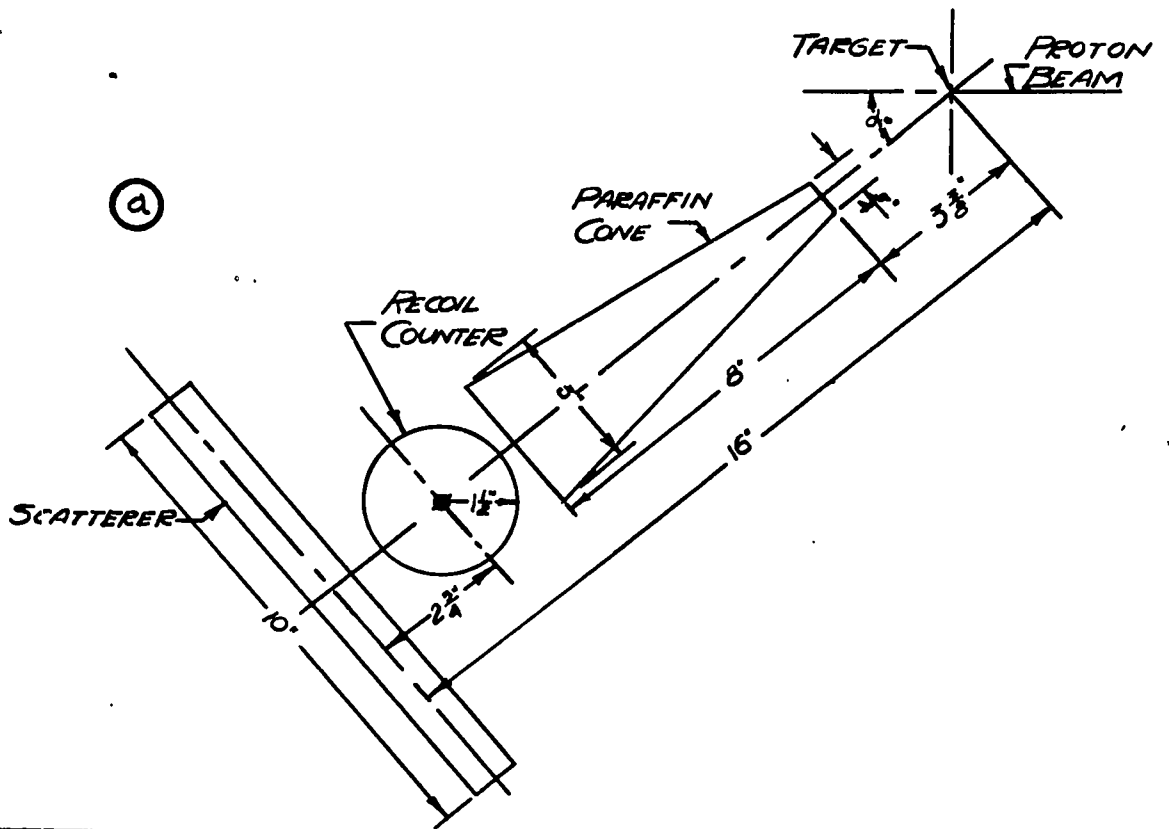
300 KEV

450 KEV

14
12
10
8
6
4
2

200 400 600 800





LEGEND	
θ	l
90°	17.26"
115°	15.27"

DOCUMENT ROOM

REC. FROM *P. Appell*

DATE *1-11-49*

REC. NO. REC. _____